DOI: 10.1002/chem.200700752

Synthesis, Aggregation and Cellular Investigations of Porphyrin–Cobaltacarborane Conjugates

Erhong Hao, Martha Sibrian-Vazquez, Wilson Serem, Jayne C. Garno,* Frank R. Fronczek, and M. Graça H. Vicente*[a]

Abstract: A new series of porphyrin-cobaltacarborane conjugates (**1**–**5**) that contain four to sixteen carborane clusters per porphyrin macrocycle, were prepared in excellent yields (90–97%) by means of a ring-opening reaction of the zwitterionic cobaltacarborane [3,3′-Co(8-$C_4H_8O_2$-1,2-$C_2B_9H_{10}$)(1′,2′-$C_2B_9H_{11}$)]. The X-ray structure of one conjugate (**3**) is presented. The aggregation properties of these conjugates were investigated by using absorption and fluorescence spectrophotometry, and the stages of microcrystal formation were captured by using atomic force microscopy. All conjugates were found to aggregate in aqueous solutions, to form a broad dispersity of particle sizes. The cellular uptake, cytotoxicity, and preferential sites of subcellular localization of this series of conjugates were evaluated in human carcinoma HEp2 cells. The extent of conjugate cellular uptake depends on the number of cobaltacarborane units at the porphyrin periphery, their distribution, and the conjugate aggregation behavior. Conjugates **2** and **4**, bearing either two adjacent or three 3,5-dicobaltacarboranephenyl groups, accumulated the most within HEp2 cells and are, therefore, the most promising boron neutron capture therapy agents. All conjugates showed very low dark- and photo-toxicity, probably due to their strong tendency for aggregation in aqueous solutions, and localized subcellularly within vesicles that correlated, to some extent, with the cell lysosomes.

Keywords: aggregation · antitumor agents · BNCT (boron neutron capture therapy) · cobaltacarborane · porphyrinoids

Introduction

Boron-containing compounds of high boron content and low toxicity have potential applications in the boron neutron capture therapy (BNCT) of cancer.[1] BNCT is an emerging binary modality for cancer treatment that involves the capture of low energy neutrons by boron-10 nuclei that are selectively localized within tumor cells. This nuclear reaction produces high linear energy transfer (high-LET) α-particles and recoiling lithium-7 nuclei, and releases about 2.4 MeV of kinetic energy.[1–3] The high-LET particles are extremely cytotoxic and have limited pathlengths in tissue (less than 10 μm). Therefore BNCT has the potential to be a highly selective tumor-targeted therapy, capable of efficiently destroying boron-10 containing tumor cells in the presence of normal boron-free cells. BNCT could particularly be useful in the treatment of high grade gliomas, malignant melanomas, meningiomas, head and neck tumors, and oral cancer.[3] Two boron-containing compounds are currently being used in BNCT clinical trials, mercapto-*closo*-dodecaborate (BSH) and 4-dihydroxyborylphenylalanine (BPA), in Europe, Japan, and in the United States. Although the clinical studies performed to date have produced evidence of a therapeutic response to BNCT, the discovery of new BNCT agents of high boron content, low toxicity, and high selectivity for tumor cells could dramatically increase the general acceptance of this cancer therapy. The amount of boron-10 needed for effective BNCT is between 20 and 30 μg of boron-10 per gram of tumor, depending upon the distribution of the boron atoms within the tumors. In order to achieve this required high boron concentration in tumors, the polyhedral borane anions, for example, *closo*-$B_{10}H_{10}^{2-}$ and *closo*-$B_{12}H_{12}^{2-}$, and the icosahedral carboranes, for example, *closo*-*o*-$C_2B_{10}H_{12}$, have been conjugated to dendrimers and various biomolecules, including nucleosides, amino acids,

[a] E. Hao, Dr. M. Sibrian-Vazquez, W. Serem, Prof. J. C. Garno, Dr. F. R. Fronczek, Prof. M. G. H. Vicente
Department of Chemistry, Louisiana State University
Baton Rouge, LA, 70803 (USA)
Fax: (+1) 225-578-3458
E-mail: jgarno@lsu.edu
vicente@lsu.edu

Supporting information for this article is available on the WWW under http://www.chemeurj.org/ or from the author.

phospholipids, monoclonal antibodies, and porphyrins.[4–9] Among these, porphyrins are very promising boron delivery vehicles because of their good tumor selectivity and long persistence within tumors.[4d,e,10] Recently, metallacarboranes, and in particular the cobaltabisdicarbollide anion $[Co(C_2B_9H_{11})_2]^-$, have received much interest[11–13] because of their high boron content, low cytotoxity,[14,15] and their remarkable stability in the presence of acids, moderate bases, radiation, and high temperature. For example, Cigler et al. recently reported that metallacarboranes are highly specific and potent inhibitors of HIV protease.[13] The discovery of a high yielding synthetic route to zwitterionic [3,3′-Co(8-$C_4H_8O_2$-1,2-$C_2B_9H_{10}$)(1′,2′-$C_2B_9H_{11}$)] has allowed its efficient conjugation to a variety of molecules.[16–20] Using this methodology, we have previously reported the conjugation of 4-hydroxyphenyl- and 4-pyridinium-porphyrins with up to four cobaltabisdicarbollide anions.[20] Herein we describe the synthesis and characterization of a new series of porphyrin-cobaltacarborane conjugates bearing between 2 and 8 cobaltabisdicarbollide anions per porphyrin macrocycle, from readily available 3,5-dihydroxyphenylporphyrins. These amphiphilic molecules contain 25–36% boron by weight and are promising new boron delivery agents for BNCT.

Results and Discussion

Synthesis of porphyrin-cobaltacarborane conjugates: Conjugates **1–5** were obtained in 90–97% yields through our previously reported methodology, by reaction of the corresponding 3,5-dihydroxyporphyrins with zwitterionic [3,3′-Co(8-$C_4H_8O_2$-1,2-$C_2B_9H_{10}$)(1′,2′-$C_2B_9H_{11}$)] in the presence of potassium carbonate.[20] As the target conjugates are poorly soluble in diethyl ether, their purification involved washing with water (to remove inorganic salts) and diethyl ether (to remove excess reacting cobaltacarborane and side products from its reaction with potassium carbonate). The 3,5-dihydroxyporphyrins **6–9** were obtained through an Adler/Longo mixed condensation of 3,5-dimethoxybenzaldehyde, benzaldehyde and pyrrole in boiling propionic acid,[21] followed by chromatographic separation and demethylation by using BBr_3 in dichloromethane.[22] Tetrakis(3,5-dihydroxyphenyl)porphyrin **10** was purchased from a commercial source and used without further purification. All conjugates are highly soluble in polar organic solvents, such as methanol, acetonitrile, acetone, ethyl acetate, DMF, and DMSO, but are poorly soluble in water. Conjugates **1–5** were characterized by HRMS (ESI-TOF), NMR, UV/Vis, and HPLC, and in the case of **3**, by X-ray crystallography. A single crystal of porphyrin **3** was obtained by recrystallization from ethyl acetate/hexane. The crystal contains two independent molecules lying on inversion centers, one of which is illustrated in Figure 1. The porphyrin core is essentially planar, with a mean deviation of 0.025 Å for its 24 atoms. The unsubstituted phenyl group forms a dihedral angle of 64.9(2)° with the porphyrin plane, and the substituted phenyl group a 79.3(3)° angle with the porphyrin. The Co atoms are coordinated in a parallel sandwich fashion by the carborane ligands. Co–B,C distances are in the range 1.969(10)–2.149(9) Å, with an average Co–C distance of 2.030 Å and an average Co–B distance of 2.095 Å. The K^+ cations are coordinated by the ethereal oxygen atoms of the side chains, as well as by ethyl acetate solvent molecules.

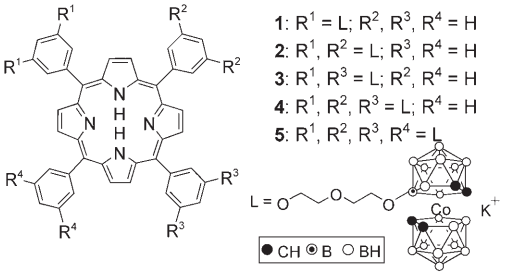

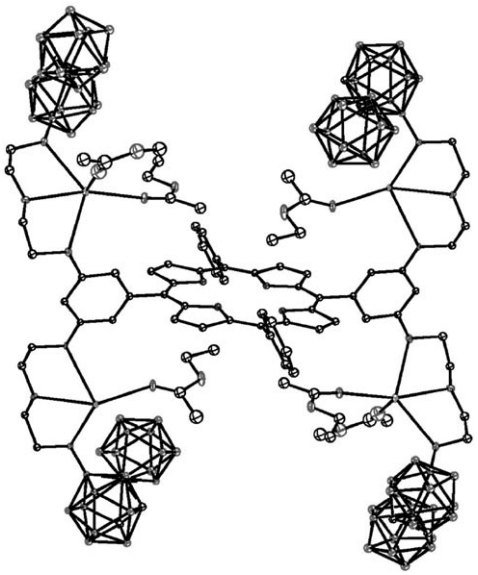

Figure 1. Molecular structure of porphyrin-cobaltacarborane conjugate **3**.

Absorption, emission and aggregation properties: Conjugates **1–5** showed similar absorption spectra to the unconjugated porphyrins **6–10** in organic solutions (see Figure 2 and Supporting Information), displaying a Soret band and four Q bands in an etio-type spectra. In addition, an absorption band at ≈314 nm corresponding to the cobaltacarborane moiety was also present (Table 1). The Soret bands for conjugates **1–5** showed a 1–2 nm red-shift with increasing number of cobaltacarborane moieties, as previously observed for a series of zwiterionic porphyrin-cobaltacarborane conjugates.[20b] The fluorescence emission spectra of conjugates **1–5** in DMSO is also typical for *meso*-tetraphenylporphyrins (Figure 3 and the Supporting Information), showing an intense band at ≈650 nm and a $\Phi_f = 0.2$ fluorescence quantum yield (Table 1). However, in HEPES (N-2-hydroxyehtylpiperazine-N′-2-ethanesulfonic acid) buffer (20 mM, pH 7.4) containing 1% DMSO (prepared by dilu-

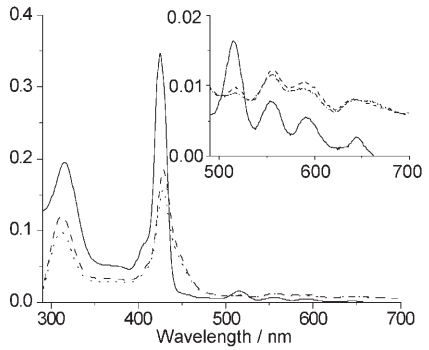

Figure 2. UV/Vis spectra of porphyrin **5** at 1×10^{-6} M in: a) DMSO solution (solid line), b) freshly prepared HEPES buffer (20 mM, pH 7.4) containing 1% DMSO (dashed line), and c) solution b after 24 h (dotted line). The inset shows amplification of the Q band region.

Table 1. Spectral properties of porphyrin-cobaltacarboranes **1**–**5** at room temperature.

	A in DMSO λ_{max} [nm][a]	A in HEPES buffer λ_{max} [nm][b]	Emission[c] λ_{max} [nm]	Φ_f[d] in DMSO
1	313, 420, 514, 551, 590, 647	312, 421, 518, 554, 595, 651	608, 652, 708	0.20
2	314, 421, 514, 550, 591, 648	316, 425, 517, 557, 594, 648	608, 651, 708	0.19
3	314, 421, 514, 551, 590, 646	316, 425, 517, 557, 601, 649	608, 651, 708	0.21
4	314, 422, 514, 550, 590, 647	313, 426, 517, 558, 594, 644	608, 651, 708	0.20
5	315, 424, 515, 554, 590, 644	312, 429, 517, 557, 594, 644	607, 650, 708	0.21

[a] 1×10^{-6} M solution in DMSO; [b] 1×10^{-6} M solution in 20 mM HEPES buffer containing 1% DMSO; [c] excitation at $\lambda=420$ nm; [d] calculated using 5,10,15,20-tetraphenylporphyrin as the standard.

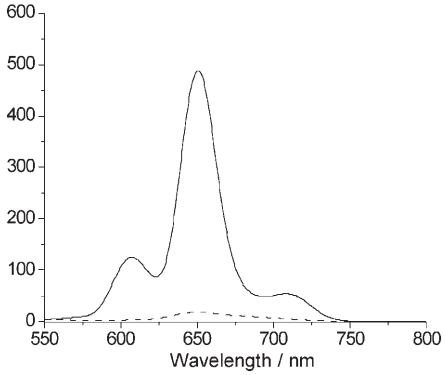

Figure 3. Fluorescence emission of porphyrin **5** at 1×10^{-6} M in: a) DMSO (solid line), and b) freshly prepared HEPES buffer (20 mM, pH 7.4) containing 1% DMSO (dashed line). Excitation at 420 nm.

tion of a DMSO stock solution into HEPES buffer), all conjugates showed red-shifted (1–5 nm) and broadened absorption bands compared with the DMSO solutions, as well as fluorescence quenching, indicating aggregation. This result was further confirmed by dynamic light scattering (DLS) and by atomic force microscopy (AFM).

The aggregation behavior of the cobaltabisdicarbollide anion[23] and of a porphyrin-cobaltacarborane conjugate[24] in aqueous solutions have recently been investigated. In agreement with these studies, we observed a marked decrease in the intensity of the Soret band in the absorption spectra of all conjugates in HEPES buffer, as well as red-shifted and broadened absorption bands, and a dramatic quench of the porphyrin fluorescence. For example the fluorescence of porphyrin-cobaltacarborane conjugate **5** in HEPES buffer was less than 1% of that in DMSO solution (Figure 3). Furthermore, the aggregation was time dependent; after 24 hours the absorption spectra of conjugate **5** in HEPES buffer showed a further decrease in the Soret band intensity and a 1 nm red-shift. Interestingly, the aggregation phenomenon is easily diagnosed, as it is often accompanied by a color change, from red (in DMSO) to green (in HEPES buffer, 20 mM, pH 7.4), even in very diluted ($\approx10^{-6}$ M) solutions. The green transparent solutions slowly become cloudy with time (over about 2 weeks), and upon sonication become transparent again. All conjugates behaved similarly, in agreement with previous studies of mono- and tetra-cobaltacarborane-substituted porphyrins.[24] In an attempt to investigate the average particle size of the aggregates by DLS we determined that the particle sizes ranged from 10 nm to 2 μm, even in freshly prepared solutions filtered through a 200 nm filter. This result indicates that the conjugates aggregate in HEPES buffer and rapidly undergo secondary aggregation. The secondary aggregated particles likely break down to the primary aggregates upon filtration or sonication.

The aggregates of conjugate **5** were visualized by AFM. An extraordinary view of the different stages of crystal growth were captured by the 8×8 μm AFM topography image (Figure 4a) for a dropcast sample of conjugate **5** dried on mica(0001). The image displays a representative morphology viewed for several areas of the surface, which was observed using several different AFM probes. Structures spanning a range of sizes have evolved as the crystals mature and grow into fractal-shaped microcrystallites. The smaller seed particles in this image have heights of 2.7 ± 0.7 nm. The lateral dimensions of the larger crystallites range in size from 0.2 to 2.5 μm. The cursor profile across several micro- and nanostructures indicates a uniform height of 2 nm. The phase image acquired at the same time indicates that the nanocrystals and microcrystallites with the brightest contrast have a consistent surface composition (Figure 4b). Phase images map out the changes in the cantilever oscillation as it is raster scanned across the surface. Changes in color contrast for the phase images result from differences in softness and adhesion, thus, all of the bright structures from nanometer to micron sizes are comprised of the same chemical material. The dark colored regions throughout the image are uncovered areas of the mica surface, and these areas are referenced as the baseline for cursor line measurements. The areas of the surface with the intermediate contrast are ascribed to residues of the HEPES matrix buffer.

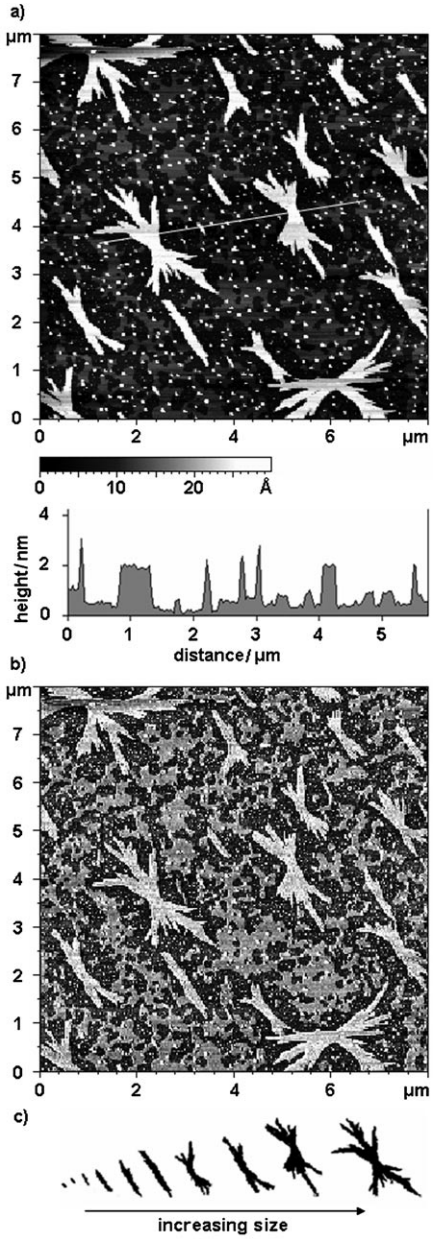

Figure 4. Crystals of conjugate **5** formed on mica(0001) viewed by: a) tapping mode AFM topography and corresponding cursor line profile, and b) simultaneously acquired phase image. Image c) shows the progressive evolution of crystallite sizes outlined from a).

The successive evolution of the stages of crystal growth can be established by organizing the changes in morphology with increasing size of aggregates. The smallest structures are the spherical seed particles, which begin to organize into linear and then columnar shapes. The linear columns then grow larger by assembling laterally into rectangular 2-D sheets. As the sheets become larger, branching takes place from the centers of the planar sheets. The thickness of the bright structures of Figure 4a corresponds to the dimensions of a single layer of porphyrins. The heights of the sheets and nanocrystals are identical, suggesting that the porphyrin crystals grow through assembly at the edges of the sheets in a planar, 2-D direction. The AFM results are in agreement with the broad dispersity of sizes measured using DLS. The morphology and transitions of crystal assembly were captured in a single AFM image to provide insight about how the conjugates aggregate. Both UV/Vis and DLS investigations yield evidence that crystals had already formed in solution. If the structures had grown from the surface then a more consistent morphology and size would have resulted. The dropcast sample preparation method, in which a droplet of porphyrin sample is placed on a surface and dried, does not typically form fractal structures. Rather, a diverse range of structures have been observed for porphyrins by AFM, depending on the sample preparation conditions and the molecular structure, such as stacks,[25] rings,[26–29] rods or needles,[30–33] and films.[34,35]

Cellular Studies: The phototoxicity, uptake and subcellular distribution of conjugates **1**–**5** were evaluated in human HEp2 cells and the results obtained are shown in Figures 5–

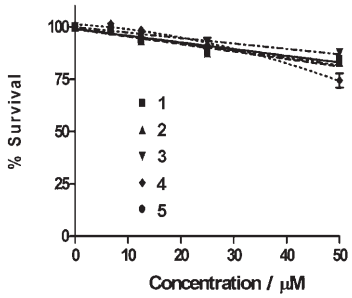

Figure 5. The phototoxicity of porphyrin conjugates conjugates **1** (full line), **2** (dash-dot-dot-dash), **3** (dash-dot-dash), **4** (dot), and **5** (dash) toward HEp2 cells using a 1 $J\,cm^{-2}$ dose of light.

7 (the dark-toxicity results and additional subcellular images are provided in the Supporting Information). Owing to the limited water solubility of all conjugates, DMSO was used as the delivery vehicle in all experiments at a concentration that never exceeded 1%. The dark- and photo-toxicity investigations were performed at concentrations up to 50 µM, as at higher concentrations the conjugates precipitated. All compounds were found to be nontoxic to the cells in the dark, up to 50 µM concentrations (see the Supporting Information). Upon exposure to a low-light dose (1 $J\,cm^{-2}$) the conjugates showed low cytotoxicity, with cell survival rates above 75% at the highest concentrations studied (Figure 5). Such low dark- and photo-toxicities are in agreement with our previous investigations of this type of compound[20b,c] and makes these conjugates of high boron content potentially promising new boron delivery agents for BNCT.

The cellular uptake of conjugates **1**–**5** depends significantly on the number of cobaltacarborane moieties at the porphyrin periphery, their distribution, amphiphilic character and aggregation behavior. Although the tetra-cobaltacarborane conjugate **3** was the most rapidly taken-up by cells at low time points, a plateau was reached after 2 hours and no significant amount of **3** was further accumulated within the cells up to 24 hours (Figure 6). In contrast, conjugate **2** (that

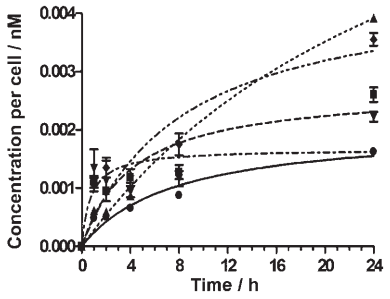

Figure 6. Time-dependent uptake of porphyrin conjugates **1** (full line), **2** (dash-dot-dot-dash), **3** (dash-dot-dash), **4** (dot), and **5** (dash) at 10 μM by HEp2 cells.

also bears four cobaltacarborane moieties, but on adjacent *meso*-phenyl groups) steadily accumulated within cells over time, and after 24 hours the amount of **2** found in cells was twice that of **3**. Similarly, conjugate **4** (that bears six cobaltacarborane moieties) was steadily taken-up by cells over time and after 24 hours it had accumulated the most within the cells out of all of the conjugates studied. It is possible that the amphiphilicity of conjugates **2** and **4**, conferred by the adjacent dicobaltacarboranylphenyl-substitution at the porphyrin periphery, enhances their affinity for lipid/aqueous interfaces and, consequently, their cellular uptake, as it has been previously observed.[20b,36] On another hand, conjugate **1** (that contains only two cobaltacarborane moieties on a *meso*-phenyl group) accumulated within the cells the slowest, and after 24 hours the amount of this conjugate found within the cells was similar to that of **3** (bearing four cobaltacarborane moieties on opposite *meso*-phenyl groups). Conjugate **5** with eight cobaltacarborane groups was rapidly taken-up by cells at short time points, but after 4 hours it accumulated more slowly within cells than **2** and **4**, possibly as a result of the formation of large aggregates, which may have decreased tendency for crossing the plasma membrane. Indeed conjugate **5** was the least soluble in aqueous solutions of all conjugates studied, despite its octa-anionic nature. Our results show, in agreement with previous studies,[24] that the delocalized negative charge on the hydrophobic cobaltacarborane substituents does not prevent the aggregation of the porphyrin molecules.

Furthermore, our results are in agreement with our previous observations that the cellular uptake of cobaltacarborane porphyrins increases with the increasing number of cobaltacarborane substituents up to four, and that conjugates with adjacent cobaltacarborane-substituted phenyl groups accumulate within cells to a higher extent than the corresponding opposite regioisomers.[20b,c] However, conjugate **5** that bears eight cobaltacarborane substituents, is not able to cross the plasma membrane as effectively as **4** and **2**, probably owing to its higher tendency to form large aggregates in aqueous solutions. It is likely that the eight hydrophobic cobaltacarborane substituents with delocalized negative charge may facilitate aggregation formation.

The intracellular distribution of this series of conjugates was investigated upon exposure of HEp2 cells to 10 μM of each conjugate for 24 hours; followed by fluorescence microscopy. We observed aggregates of all conjugates within the cells and as a result the porphyrin fluorescence signal was weak. All conjugates showed a punctuate pattern, as shown in Figure 7 for conjugate **4** (see Supporting Information for similar images obtained for **1**–**3** and **5**). Co-localization investigations using BODIPY Ceramide, LysoSensor Green, and MitoTracker Green suggest that the conjugates localize partially within the cell lysosomes, but not in the Golgi nor the mitochondria. Some of the conjugate aggregated species seem to remain trapped in vesicles that correlate to some extent to the cell lysosomes (Figure 7f). These results are in agreement with previous reports showing that anionic carboranyl-containing porphyrins localize preferentially within the cell lysosomes.[20b,c,37]

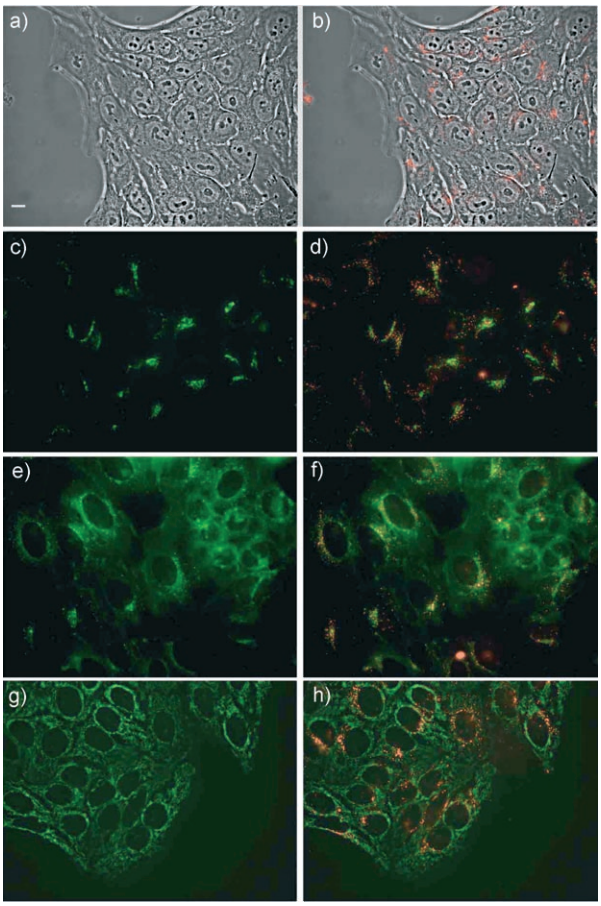

Figure 7. Subcellular localization of conjugate **4** in HEp2 cells at 10 μM for 24 h. a) Phase contrast, b) overlay of **4** fluorescence with phase contrast, c) BODIPY Ceramide fluorescence, e) LysoSensor Green fluorescence, and g) MitoTracker Green fluorescence. Overlays of organelle tracers with **4** fluorescence (d, f, and h). Scale bar: 10 μm.

Conclusion

A new series of porphyrin-cobaltacarborane conjugates containing 2 to 8 cobaltacarborane moieties per porphyrin molecule have been synthesized in excellent yields from readily

available starting materials. All conjugates form aggregates in aqueous solutions as determined by using DLS and AFM, and UV/Vis and fluorescence spectroscopies. In particular, conjugate **5** produces 3-D crystallites over time, which were visualized by AFM. The preferential sites of subcellular localization of these conjugates in human HEp2 cells are the lysosomes, probably as a result of their anionic nature and aggregate formation. The cellular uptake of this series of conjugates depends on the number of cobaltacarborane moieties at the porphyrin periphery, their distribution, amphiphilic character, and aggregation properties. Conjugates **2** and **4**, bearing two adjacent and three 3,5-dicobaltacarboranephenyl groups, respectively, accumulated the most within HEp2 cells, showed very low dark- and photo-toxicity and are, therefore, the most promising BNCT agents.

Experimental Section

Syntheses: All reactions were monitored by TLC by means of 0.25 mm silica gel plates with or without UV indicator (60F-254). Silica gel Sorbent Technologies 32–63 μm was used for flash column chromatography. HPLC analyses were performed on a Dionex system including a P680 pump and a UVD340U detector, using a Delta Park C_{18} 300 Å, 5 μm, 3.9×150 mm (Waters) column and a stepwise gradient with a 1 mL min^{-1} flow rate, 20 μL injected volume and wavelength detection at 250 and 420 nm. Two solvent systems were used: a) stepwise gradient from 65% B to 95% B in 30 min, then 95% B for 5 min, and then from 95% B back to 65% B in 2 min (A: 10 mM BIS-TRIS propane buffer (pH 7.0) with 5 mM tetraethylammonium bromide as ion-pair reagent; B: acetonitrile); b) stepwise gradient from 85% to 95% buffer B in 15 min, then 95% B for 15 min, and then from 95% B back to 85% B in 7 min (A: 5% acetonitrile in 0.1% TFA, H_2O; B: 5% H_2O, 0.1% TFA in acetonitrile). ^{1}H- and ^{13}C NMR were obtained by using either a DPX-250 or a ARX-300 Bruker spectrometer. Chemical shifts (δ) are given in ppm relative to [D6]acetone (^{1}H: 2.05 ppm, ^{13}C: 206.0 ppm) unless otherwise indicated. Mass spectra were obtained by using ESI-TOF with the negative mode on an Applied Biosystems QSTAR XL. The isotope peaks were matched with calculated patterns; only the most abundant peaks for each porphyrin are listed below. The isotope distributions for porphyrins **1–5** in comparison with the calculated distributions are shown in the Supporting Information. All solvents were obtained from Fisher Scientific (HPLC grade) and used without further purification. [3,3′-Co(8-$C_4H_8O_2$–1,2-$C_2B_9H_{10}$)(1′,2′-$C_2B_9H_{11}$)] was prepared as previously described in the literature.[17b]

Porphyrin synthesis: 5-(3,5-dimethoxyphenyl)-10,15,20-triphenylporphyrin, 5,10-di(3,5-dimethoxyphenyl)-15,20-diphenylporphyrin, 5,15-di(3,5-dimethoxyphenyl)-10,20-diphenylporphyrin, and 5,10,15-tri(3,5-dimethoxyphenyl)-20-phenylporphyrin were synthesized by the condensation of benzaldehyde, 3,5-dimethoxybenzaldehyde, and pyrrole in refluxing propionic acid.[21] The reaction mixture was cooled to −20 °C, the precipitate was filtered and then washed with methanol. The porphyrin residue was purified by means of flash column chromatography on silica gel by using CH_2Cl_2 for elution. The methoxyl groups were cleaved as described in the literature[22] to afford the corresponding 3,5-dihydroxyphenylporphyrins **6–9**.

5-(3,5-Dihydroxyphenyl)-10,15,20-triphenylporphyrin 6: This porphyrin was obtained in 89.3% yield and its spectroscopic data are in full agreement with that reported in the literature.[22]

5,10-Di(3,5-dihydroxyphenyl)-15,20-diphenylporphyrin 7: This porphyrin was obtained in 91.9% yield. ^{1}H NMR ([D6]acetone): δ= 9.05 (d, J= 4.1 Hz, 4H; β-H), 8.84 (m, 4H; β-H), 8.71 (s, 4H; OH), 8.22 (m, 4H; *o*-phenyl-H), 7.80 (m, 6H; *m*,*p*-phenyl-H), 7.27 (d, J=1.7 Hz, 4H; *o*-Ar-H), 6.85 (d, J=4.6 Hz, 2H; *p*-Ar-H), −2.76 ppm (s, 2H; NH); MS(MALDI-TOF): *m*/*z*: calcd for $C_{44}H_{30}N_4O_4$: 679.234; found: 679.148 [*M*+H]$^+$.

5,15-Di(3,5-dihydroxyphenyl)-10,20-diphenylporphyrin 8: This porphyrin was obtained in 89.4% yield. ^{1}H NMR ([D6]acetone): δ=9.04 (d, J= 4.1 Hz, 4H; β-H), 8.85 (d, J=4.1 Hz, 4H; β-H), 8.70 (s, 4H; OH), 8.25 (m, 4H; *o*-phenyl-H), 7.83 (m, 6H; *m*,*p*-phenyl-H), 7.25 (d, J=1.8 Hz, 4H; *o*-Ar-H), 6.83 (t, J=3.6 Hz, 2H; *p*-Ar-H), −2.77 ppm (s, 2H; NH); MS(MALDI-TOF): *m*/*z*: calcd for $C_{44}H_{30}N_4O_4$: 679.234; found: 679.076 [*M*+H]$^+$.

5,10,15-Tri(3,5-dihydroxyphenyl)-20-phenylporphyrin 9: This porphyrin was obtained in 90.5% yield. ^{1}H NMR ([D6]acetone): δ=9.04 (d, J= 4.3 Hz, 6H; β-H), 8.84 (d, J=4.5 Hz, 2H; β-H), 8.70 (s, 6H; OH), 8.24 (m, 2H; *o*-phenyl-H), 7.83 (m, 3H; *m*,*p*-phenyl-H), 7.25 (t, J=3.6 Hz, 6H; *o*-Ar-H), 6.84 (m, 3H; *p*-Ar-H), −2.76 ppm (s, 2H; NH); MS(MALDI-TOF): *m*/*z*: calcd for $C_{44}H_{30}N_4O_6$: 711.224; found: 711.222 [*M*+H]$^+$.

Porphyrin conjugate 1: Porphyrin **6** (32.3 mg, 0.05 mmol) and K_2CO_3 (28.5 mg, 0.21 mmol) in acetone (10 mL) were heated to 60 °C under argon for 15 min. After cooling the reaction mixture to room temperature [3,3′-Co(8-$C_4H_8O_2$–1,2-$C_2B_9H_{10}$)(1′,2′-$C_2B_9H_{11}$)] (41.2 mg, 0.10 mmol) was added, the reaction mixture stirred at room temperature for 2 h and then refluxed overnight. A second portion of [3,3′-Co(8-$C_4H_8O_2$-1,2-$C_2B_9H_{10}$(1′,2′-$C_2B_9H_{10}$)] (41.2 mg, 0.1 mmol) was added and heating continued for 24 h. The mixture was cooled to room temperature, the solvent removed under vacuum, and the residue dissolved in ethyl acetate. The organic phase was washed with water, dried over anhydrous Na_2SO_4, and the solvent removed under vacuum. Purification by column chromatography on silica gel using ethyl acetate/acetone 5:1 for elution gave the title porphyrin conjugate (75.1 mg) in 97.2% yield. HPLC t_R=5.97; ^{1}H NMR ([D6]acetone): δ=9.06 (d, J=4.1 Hz, 2H; β-H), 8.87 (m, 6H; β-H), 8.26 (m, 6H; *o*-phenyl-H), 7.84 (m, 9H; *m*,*p*-phenyl-H), 7.49 (d, J=2.2 Hz, 2H; *o*-Ar-H), 7.08 (m, 2H; *p*-Ar-H), 4.40 (br t, 4H; OCH_2), 4.23 (br t, 8H; OCH_2), 3.92 (br t, 4H; OCH_2), 3.66 (s, 8H; carborane-CH), 1.6–3.0 (br, 34H; BH), −2.76 ppm (s, 2H; NH); ^{13}C NMR ([D6]acetone): δ= 159.1, 144.4, 142.8, 135.1, 128.6, 127.6, 120.8, 120.7, 115.3, 101.8, 72.8, 70.1, 69.1, 68.7, 54.7, 47.1 ppm; UV/Vis (acetone) λ_{max}=415 (ε 318,600), 511 (14,000), 544 (5,400), 589 (3,800), 646 nm (3,200); HRMS(ESI): *m*/*z*: calcd for $C_{60}H_{85}N_4O_6B_{36}Co_2$: 732.9379; found: 732.9421.

Porphyrin conjugate 2: Porphyrin **7** (17.2 mg, 0.025 mmol) and K_2CO_3 (28.1 mg, 0.20 mmol) in acetone (10 mL) were heated to 60 °C under argon for 15 min as described above. [3,3′-Co(8-$C_4H_8O_2$–1,2-$C_2B_9H_{10}$)(1′,2′-$C_2B_9H_{11}$)] was added in three portions (60.3, 11.0 and 10.3 mg). The title porphyrin conjugate was obtained (57.1 mg, 0.023 mmol) after washing with diethyl ether and drying, in 91.3% yield. HPLC t_R=12.22; ^{1}H NMR ([D6]acetone): δ=8.99 (s, 4H; β-H), 8.81 (m, 4H; β-H), 8.22 (m, 4H; *o*-phenyl-H), 7.80 (m, 6H; *m*,*p*-phenyl-H), 7.45 (d, J=1.6 Hz, 4H; *o*-Ar-H), 7.05 (s, 2H; *p*-Ar-H), 4.37 (m, 8H; OCH_2), 4.15 (s, 16H; OCH_2), 3.91 (m, 8H; OCH_2), 3.64 (s, 16H; carborane-CH), 1.6–3.0 (br, 68H; BH), −2.81 ppm (s, 2H; NH); ^{13}C NMR ([D6]acetone): δ=159.1, 144.5, 142.7, 135.1, 128.6, 127.5, 120.9, 120.6, 115.2, 101.8, 72.9, 70.1, 69.1, 68.7, 54.4, 47.2 ppm; UV/Vis (acetone) λ_{max}= 417 (ε 421,500), 512 (19,500), 546 (5,500), 588 (4,300), 645 nm (2,900); HRMS(ESI): *m*/*z*: calcd for $C_{76}H_{141}N_4O_{12}B_{72}Co_4$: 579.3782; found: 579.3815.

Porphyrin conjugate 3: Porphyrin **8** (34.2 mg, 0.05 mmol) and K_2CO_3 (54.9 mg, 0.40 mmol) in acetone (20 mL) were heated to 60 °C under argon for 15 min, as described above. [3,3′-Co(8-$C_4H_8O_2$–1,2-$C_2B_9H_{10}$)(1′,2′-$C_2B_9H_{11}$)] was added in three portions (82.2, 20.0 and 20.1 mg). The title porphyrin conjugate was obtained (111.4 mg) in 89.8% yield after washing with diethyl ether and drying. HPLC t_R= 15.16; ^{1}H NMR ([D6]acetone): δ=9.02 (d, J=4.5 Hz, 4H; β-H), 8.86 (d, J=4.6 Hz, 4H; β-H), 8.27 (m, 4H; *o*-phenyl-H), 7.84 (m, 6H; *m*,*p*-phenyl-H), 7.50 (s, 4H; *o*-Ar-H), 7.08 (s, 2H; *p*-Ar-H), 4.41 (br t, 8H; OCH_2), 4.19 (s, 16H; OCH_2), 3.94 (br t, 8H; OCH_2), 3.68 (s, 16H; carborane-CH), 1.6–3.0 (br, 68H; BH), −2.77 ppm (s, 2H; NH); ^{13}C NMR ([D6]acetone): δ=159.1, 144.5, 142.7, 135.1, 128.6, 127.6, 120.8, 120.7, 115.2, 101.7, 72.8, 70.1, 69.1, 68.6, 54.4, 47.2; UV/Vis (acetone) λ_{max}=417 (ε 495,700), 512 (23,000), 546 (9,100), 588 (4,300), 645 nm (5,600); HRMS(ESI): *m*/*z*: calcd for $C_{76}H_{141}N_4O_{12}B_{72}Co_4$: 579.3782; found: 579.3838.

Crystal data for 3: Dark orange-brown, $K_4[C_{76}H_{142}B_{72}N_4O_{12}Co_4]\cdot 7(C_4H_8O_2)$, $M_r = 3091.1$, triclinic space group $P\bar{1}$, $a = 16.476(2)$, $b = 22.049(3)$, $c = 23.980(3)$ Å, $\alpha = 75.532(7)$, $\beta = 74.298(7)$, $\gamma = 88.641(8)°$, $V = 8111.4(18)$ Å^3, $Z = 2$, $\rho_{calcd} = 1.266$ gcm^{-3}, $Mo_{K\alpha}$ radiation ($\lambda = 0.71073$ Å; $\mu = 0.566$ mm^{-1}), $T = 110$ K, 79142 data by Nonius KappaCCD, $R = 0.101$ ($F^2 > 2\sigma$), $Rw = 0.308$ (all F^2) for 23114 unique data having $\theta < 23.3°$ and 1777 refined parameters. There are two independent molecules in the asymmetric unit, both lying on inversion centers. One of them is associated with six ethyl acetate molecules, the other, eight. Because of limited crystal quality, it was not possible to refine all solvent atoms anisotropically. The N–H hydrogen atoms were not located. Crystallographic data have been deposited with the Cambridge Crystallographic Data Centre as supplementary publication no. CCDC 644477. Copies if the data can be obtained, free of charge, on application to CCDC, 12 Union Road, Cambridge, CB2 1EZ, UK, (fax: +44-(0)1223–336033 or e-mail: deposit@ccdc.cam.ac.uk).

Porphyrin conjugate 4: Porphyrin **9** (11.8 mg, 0.017 mmol) and K_2CO_3 (28.0 mg, 0.20 mmol) in acetone (10 mL) were heated to 60 °C under argon for 15 min, as described above. [3,3′-Co(8-$C_4H_8O_2$–1,2-$C_2B_9H_{10}$)(1′,2′-$C_2B_9H_{11}$)] was added in three portions (42.0, 21.0 and 21.0 mg). The title porphyrin conjugate was obtained (52.8 mg) in 93.4% yield after washing with diethyl ether and drying. HPLC $t_R = 11.68$; ^{1}H NMR ([D6]acetone): $\delta = 9.00$ (s, 6H; β-H), 8.85 (d, $J = 4.0$ Hz, 2H; β-H), 8.26 (m, 2H; *o*-phenyl-H), 7.84 (m, 3H; *m*,*p*-phenyl-H), 7.48 (s, 6H; *o*-Ar-H), 7.08 (s, 3H; *p*-Ar-H), 4.40 (br t, 12H; OCH_2), 4.18 (s, 24H; OCH_2), 3.94 (br t, 12H; OCH_2), 3.68 (s, 24H; carborane-CH), 1.6–3.0 (br, 102H; BH), −2.81 ppm (s, 2H; NH); ^{13}C NMR ([D6]acetone): $\delta =$ 159.1, 144.5, 142.7, 135.1, 128.6, 127.5, 120.9, 120.6, 115.2, 101.8, 72.9, 70.1, 69.1, 68.7, 54.4, 47.2 ppm; UV/Vis (acetone) $\lambda_{max} = 418$ (ε 396,100), 512 (19,500), 546 (7,400), 588 (7,200), 644 nm (4,700); HRMS(ESI): *m*/*z*: calcd for $C_{92}H_{199}N_4O_{18}B_{708}Co_6$: 528.3596; found: 528.3658.

Porphyrin conjugate 5: Porphyrin **10** (18.9 mg, 0.025 mmol) and K_2CO_3 (500.0 mg, 3.62 mmol) in acetone (20 mL) were heated to 60 °C under argon for 15 min, as described above. [3,3′-Co(8-$C_4H_8O_2$–1,2-$C_2B_9H_{10}$)(1′,2′-$C_2B_9H_{11}$)] was added in three portions (100.0, 40.0 and 21.0 mg). The title porphyrin conjugate was obtained (104.2 mg) in 94.5% yield after washing with diethyl ether and drying. HPLC $t_R = 5.66$; ^{1}H NMR ([D6]acetone): $\delta = 8.99$ (s, 8H; β-H), 7.45 (s, 8H; *o*-Ar-H), 7.08 (s, 4H; *p*-phenyl-H), 4.39 (br t, 16H; OCH_2), 4.21 (br, 32H; OCH_2), 3.93 (br t, 16H; OCH_2), 3.68 (s, 32H; carborane-CH), 1.6–3.0 (br, 136H; BH), −2.82 ppm (s, 2H; NH); ^{13}C NMR ([D6]acetone): $\delta = 159.5$, 144.9, 121.0, 115.6, 102.3, 73.2, 70.6, 70.2, 69.6, 55.0, 47.6 ppm. UV/Vis (acetone) $\lambda_{max} = 419$ (ε 425,200), 512 (21,700), 546 (7,200), 587 (7,200), 645 nm (4,000); HRMS(ESI): *m*/*z*: calcd for $C_{108}H_{255}N_4O_{24}B_{144}Co_8$: 502.8503; found: 502.8544.

Photophysical Studies: Electronic absorption spectra were measured by means of a UV/Vis spectrophotometer equipped with a photodiode detector, in the 200–700 nm wavelength range with 0.1 nm accuracy. Fluorescence spectra were measured on a luminescence spectrophotometer equipped with a Xenon lamp, in the 500–800 nm wavelength range with 1 nm accuracy. The fluorescence quantum yields were measured by using the standard method and 5,10,15,20-tetraphenylporphyrin as the standard (quantum yield is 0.11), according to the literature.[38] The 1×10^{-6} M solutions of conjugates **1**–**5** in 20 mM HEPES buffer (pH 7.4) containing 1% DMSO were prepared by adding 100 mL of 1×10^{-4} M stock solutions in DMSO to 10 mL of HEPES buffer (20 mM, pH 7.4).

AFM Studies: *Sample preparation*: Porphyrin samples were first dissolved in DMSO, and then added at 1% vol/vol to HEPES buffer (20 mM). A 10 μL drop of the porphyrin solution (1×10^{-6} M) was deposited onto freshly cleaved mica(0001) by using a micropipette. The samples were dried in air at room temperature for 12 h before AFM imaging. AFM images were acquired by using an Agilent 5500 AFM/SPM system (Tempe, AZ) operated in tapping mode, with Picoscan v5.3.3 software. Rectangular cantilevers (NSC15/Cr-Au BS) from MikroMasch (Wilsonville, Oregon) were used for imaging porphyrin structures on mica. These probes have relatively high force constants ($k_{avg} = 40$ N/m) and resonance frequency of 325 kHz. The tapping mode probe used for sample characterization was oscillated near its resonance frequency at 324.9 kHz in an ambient environment.

Cell Culture: All tissue culture media and reagents were obtained from Invitrogen. Human HEp2 cells were obtained from ATCC and maintained in a 50:50 mixture of DMEM (Dulbecco's Modified Eagel's Medium): Advanced MEM (Minimum Essential Medium) containing 5% FBS (fetal bovine serum). The cells were sub-cultured biweekly to maintain sub-confluent stocks.

Time-dependent cellular uptake: The HEp2 cells were plated at 10000 per well in a Costar 96 well plate and allowed to grow for 36 h. Porphyrin stocks **1**–**5** were prepared in DMSO at a concentration of 10 mM and then diluted into medium to final working concentrations. The cells were exposed to 10 μM of each porphyrin conjugate for 0, 1, 2, 4, 8, and 24 h. At the end of the incubation time the loading medium was removed and the cells were washed with 200 μL of PBS (phosphate buffered saline). The cells were solubilized upon addition of 100 μL of 0.25% Triton X-100 (Calbiochem) in PBS. To determine the porphyrin concentration, fluorescence emission was read at 410/650 nm (excitation/emission) by using a BMG FLUOstar plate reader. The cell numbers were quantified by using the CyQuant reagent (Molecular Probes).

Dark cytotoxicity: The HEp2 cells were plated as described above and allowed 36–48 h to attach. The cells were exposed to increasing concentrations of porphyrin conjugate up to 50 μM and incubated overnight. The loading medium was then removed and medium containing Cell Titer Blue (Promega) as per manufacturer's instructions was added to the cells. Cell viability was then measured by reading the fluorescence at 520/584 nm using a BMG FLUOstar plate reader. The signal was normalized to 100% viable (untreated) cells and 0% viable (treated with 0.2% saponin) cells.

Phototoxicity: The HEp2 cells were prepared as described above for the dark cytotoxicity assay and treated with porphyrin conjugate concentrations of 0, 6.25, 12.5, 25, and 50 μM. After compound loading, the medium was removed and replaced with a medium containing 50 mM HEPES pH 7.4. The cells were then placed on ice and exposed to light from a 100 W halogen lamp filtered through a 610 nm long pass filter (Chroma) for 20 min. An inverted plate lid filled with water to a depth of 5 mm acted as an IR filter. The total light dose was approximately 1 J cm^{-2}. The cells were returned to the incubator overnight and assayed for viability as described above for the dark cytotoxicity experiment.

Microscopy: The HEp2 cells were plated on LabTek 2 chamber coverslips and incubated for 24–36 H; before being exposed to 10 μM of each porphyrin conjugate. For the co-localization experiments the cells were incubated for 24 h concurrently with the porphyrin conjugate and one of the following organelle tracers, for 30 min: MitoTracker Green at 250 nM (mitochondria), LysoSensor Green at 50 nM (lysosomes), BODIPY FL C_5-ceramide at 50 nM (Golgi network). The slides were washed three times with growth medium and a new medium containing 50 mM HEPES pH 7.4 was added. The fluorescent microscopy was performed by using a Zeiss Axiovert 200 M inverted fluorescence microscope fitted with standard FITC and Texas Red filter sets (Chroma). The images were acquired with a Zeiss Axiocam MRM CCD camera fitted to the microscope.

Supporting Information for this article is available on the WWW under http://www.chemeurj.org/or from the author. It contains additional UV/Vis and fluorescence spectra, dark cytotoxicity data, subcellular localization images, the size distribution of crystal seeds within the AFM image, HPLC traces and conditions, MS and ^{1}H NMR spectra.

Acknowledgements

The authors wish to thank Vijay Gottumukkala for preliminary cellular investigations and Erick Soto-Cantu for assistance with the DLS measurements. This work was supported by the National Institute of Health, grant R01 CA098902 (MGHV), and by the American Chemical Society Petroleum Research Fund PRF G43352-G5 (JCG).

[1] A. H. Soloway, W. Tjarks, B. A. Barnum, F. G. Rong, R. F. Barth, I. M. Codogni, J. G. Wilson, *Chem. Rev.* **1998**, *98*, 1515–1562.
[2] R. F. Barth, J. A. Coderre, M. G. H. Vicente, T. E. Blue, *Clin. Cancer Res.* **2005**, *11*, 3987–4002.
[3] R. F. Barth, H. Joensuu, *Radiol. Oncol.* **2007**, 82, 119–122.
[4] a) V. I. Bregadze, I. B. Sivaev, S. A. Glazun, *Curr. Med. Chem. Anti-Cancer Agents* **2006**, *6*, 75–109; b) G. W. Kabalka, M.-L. Yao, *Curr. Med. Chem. Anti-Cancer Agents* **2006**, *6*, 111–125; c) Y. Byun, S. Narayanasamy, J. Johnsamuel, A. K. Bandy-Opadhyaya, R. Tiwari, A. S. Al-Madhoun, R. F. Barth, S. Eriksson, W. Tjarks, *Curr. Med. Chem. Anti-Cancer Agents* **2006**, *6*, 127–144; d) M. W. Renner, M. Miura, M. W. Easson, M. G. H. Vicente, *Curr. Med. Chem. Anti-Cancer Agents* **2006**, *6*, 145–157; e) M. Ratajski, J. Osterloh, D. Gabel, *Curr. Med. Chem. Anti-Cancer Agents* **2006**, *6*, 159–166; f) G. Wu, R. F. Barth, W. Yang, R. J. Lee, W. Tjarks, M. V. Backer, J. M. Backer, *Curr. Med. Chem. Anti-Cancer Agents* **2006**, *6*, 167–184.
[5] M. C. Parrott, E. B. Marchington, J. F. Valliant, A. Adronov, *J. Am. Chem. Soc.* **2005**, *127*, 12081–12089.
[6] K. M. Galie, A. Mollard, I. Zharov, *Inorg. Chem.* **2006**, *45*, 7815–7820.
[7] L. Ma, J. Hamdi, F. Wong, M. F. Hawthorne, *Inorg. Chem.* **2006**, *45*, 278–285.
[8] H. Nakamura, M. Ueno, J. Lee, H. S. Ban, E. Justus, P. Fan, D. Gabel, *Tetrahedron Lett.* **2007**, *48*, 3151–3154.
[9] C. Di Meo, L. Panza, D. Capitani, L. Mannina, A. Banzato, M. Rondina, D. Renier, A. Rosato, V. Crescenzi, *Biomacromolecules* **2007**, *8*, 552–559.
[10] J. Osterloh, M. G. H. Vicente, *J. Porphyrins Phthalocyanines* **2002**, *6*, 305–324.
[11] I. B. Sivaev, V. I. Bregadze, *J. Organomet. Chem.* **2000**, *614–615*, 27–36.
[12] a) A. B. Olejniczak, J. Plesek, O. Kriz, Z. J. Lesnikowski, *Angew. Chem. Int. Ed.* **2003**, *42*, 5740–5743; b) Z. J. Lesnikowski, E. Paradowska, A. B. Olejniczak, M. Studzinska, P. Seekamp, U. Schussler, D. Gabel, R. F. Schinazi, J. Plesek, *Bioorg. Med. Chem.* **2005**, *13*, 4168–4175; c) A. B. Olejniczak, J. Plesek, Z. J. Lesnikowski, *Chem. Eur. J.* **2007**, *13*, 311–318.
[13] P. Cigler, M. Kozisek, P. Rezacova, J. Brynda, Z. Otwinowski, J. Pokorna, J. Plesek, B. Gruner, L. Doleckova-Maresova, M. Masa, J. Sedlacek, J. Bodem, H-G. Krausslich, V. Kral, J. Konvalinka, *Proc. Natl. Acad. Sci. USA* **2005**, *102*, 15394–15399.
[14] R. Makrlik, P. Vanura, *Talanta* **1985**, *32*, 423–429.
[15] a) R. A. Spryshkova, V. A. Brattsev, T. L. Sherman, V. I. Stanko, *Med. Radiol.* **1981**, *26*, 7, 51–55; b) R. A. Spryshkova, L. I. Karaseva, V. A. Brattsev, N. G. Serebriakov, *Med. Radiol.* **1981**, *26*, 6, 62–64.
[16] a) J. Plešek, S. Heřmánek, K. Baše, L. Todd, W. F. Wright, *Collect. Czech. Chem. Commun.* **1976**, *41*, 3509–3515; b) V. Šubrtová, V. Petřicek, A. Linek, *Z. Kristallogr.* **1976**, *144*, 139–141; c) J. Plešek, S. Heřmánek, A. Franken, I. Cisarova, C. Nachtigal, *Collect. Czech. Chem. Commun.* **1997**, *62*, 47–56; d) J. Plesek, B. Gruner, S. Hermanek, J. Baca, V. Marecek, J. Janchenova, A. Lhotsky, K. Holub, P. Selucky, J. Rais, I. Cisarova, J. Caslavsky, *Polyhedron* **2002**, *21*, 975–986.
[17] a) I. B. Sivaev, Z. A. Starikova, S. Sjoberg, V. I. Bregadze, *J. Organomet. Chem.* **2002**, *649*, 1–8; b) F. Teixidor, J. Pedrajas, I. Rojo, C. Vinas, R. Kivekas, R. Sillanpaa, I. Sivaev, V. Bregadze, S. Sjoberg, *Organometallics* **2003**, *22*, 3414–3423.
[18] T. Peymann, K. Kuck, D. Gabel, *Inorg. Chem.* **1997**, *36*, 5138–5139.
[19] J. Llop, C. Masalles, C. Vinas, F. Teixidor, R. Sillanpaa, R. Kivekas, *Dalton Trans.* **2003**, 556–561.
[20] a) E. Hao, M. G. H. Vicente, *Chem. Commun.* **2005**, 1306–1308; b) E. Hao, T. J. Jensen, B. H. Courtney, M. G. H. Vicente, *Bioconjugate Chem.* **2005**, *16*, 1495–1502; c) M. Sibrian-Vazquez, E. Hao, T. J. Jensen, M. G. H. Vicente, *Bioconjugate Chem.* **2006**, *17*, 928–934.
[21] L. Jiao, E. Hao, F. R. Fronczek, K. M. Smith, M. G. H. Vicente, *Tetrahedron* **2007**, *63*, 4011–4017.
[22] T. Tanaka, K. Endo, Y. Aoyama, *Bull. Chem. Soc. Jpn.* **2001**, *74*, 907–916.
[23] P. Matejicek, P. Cigler, K. Prochazka, V. Kral, *Langmuir* **2006**, *22*, 575–581.
[24] P. Kubat, K. Lang, P. Cigler, M. Kozisek, P. Matejicek, P. Janda, Z. Zelinger, K. Prochazka, V. Kral, *J. Phys. Chem. B* **2007**, *111*, 4539–4546.
[25] C. M. Drain, T. Milic, J. C. Garno, G. Smeureanu, J. D. Batteas, *Polym. Prepr. Am. Chem. Soc. Div. Polym. Chem. Polymer Preprints* **2004**, *45*, 346–347.
[26] S. C. Doan, S. Shanmugham, D. E. Aston, J. L. McHale, *J. Am. Chem. Soc.* **2005**, *127*, 5885–5892.
[27] P. Foubert, P. Vanoppen, M. Martin, T. Gensch, J. Hofkens, A. Helser, A. Seeger, R. M. Taylor, A. E. Rowan, R. J. M. Nolte, F. C. De Schryver, *Nanotechnology* **2000**, *11*, 16–23.
[28] H. Zhang, Y. Ma, Z. H. Lu, Z. Z. Gu, *Colloids Surf., A* **2005**, *257–258*, 291–294.
[29] C. R. L. P. N. Jeukens, M. C. Lensen, F. J. P. Wijnen, J. A. A. W. Elemans, P. C. M. Christianen, A. E. Rowan, J. W. Gerritsen, R. J. M. Nolte, J. C. Maan, *Nano Lett.* **2004**, *4*, 1401–1406.
[30] H. George, R. E. Palmer, Q. Guo, N. Bampos, J. K. M. Sanders, *Surf. Sci.* **2006**, *600*, 3274–3279.
[31] V. Snitka, M. Rackaitis, R. Rodaite, *Sens. Actuators B* **2005**, *109*, 159–166.
[32] C. Ikeda, E. Fujiwara, A. Satake, Y. Kobuke, *Chem. Commun.* **2003**, 616–617.
[33] A. D. Schwab, D. E. Smith, B. Bond-Watts, D. E. Johnston, J. Hone, A. T. Johnson, J. C. dePaula, W. F. Smith, *Nano Lett.* **2004**, *4*, 1261–1265.
[34] P. Sun, D. A. Jose, A. D. Shukla, J. J. Shukla, A. Das, J. F. Rathman, P. Ghosh, *Langmuir* **2005**, *21*, 3413–3423.
[35] X. L. Li, W. Q. Xu, T. Itoh, A. Ikehata, B. Zhao, B. F. Li, Y. Ozaki, *J. Colloid Interface Sci.* **2005**, *284*, 582–592.
[36] B. W. Henderson, D. A. Bellnier, W. R. Greco, A. Sharma, R. K. Pandey, L. A. Vaughan, K. R. Weishaupt, T. J. Dougherty, *Cancer Res.* **1997**, *57*, 4000–4007.
[37] V. Gottumukkala, R. Luguya, F. R. Fronczek, M. G. H. Vicente, *Bioorg. Med. Chem.* **2005**, *13*, 1633–1640.
[38] S. Fery-Forgues, D. Lavabre, *J. Chem. Educ.* **1999**, *76*, 1260–1264.

Received: May 17, 2007
Published online: August 3, 2007

